RBRH

Revista Brasileira de Recursos Hídricos
Brazilian Journal of Water Resources
Versão On-line ISSN 2318-0331
RBRH, Porto Alegre, v. 30, e20, 2025
Scientific/Technical Article

https://doi.org/10.1590/2318-0331.302520240009

An empirical method to identify breaking waves

Um método empírico para identificar arrebentação de ondas

Mauricio Felga Gobbi[1]

[1]Universidade Federal do Paraná, Curitiba, PR, Brasil
E-mail: gobbi@ufpr.br (MFG)

Received: February 21, 2024 - Revised: May 21, 2024 - Accepted: March 07, 2025

ABSTRACT

In this paper we propose a method to identify breaking waves in shallow water. The method takes the local surface elevation time series and creates a new time series computed from the local energy spectrum using the wavelet transform of the input signal which quantifies the frequencies typically present in breaking waves. A laboratory experiment in a random wave flume was conducted and used to test the method in three positions along the tank, where: (a) no waves were breaking; (b) about 30% of the waves were breaking; (c) and nearly all waves were breaking. The method was statistically tested for its ability to correctly identify breaking waves, using the fact that all waves passing the gauge locations along the shoaling process were visually identified and marked as breaking or nonbreaking. The method proved itself accurate for most cases, and only misses when waves are on the verge of breaking.

Keywords: Wave breaking; Random waves; Wavelet analysis; Coastal processes.

RESUMO

Neste artigo é proposto um método para identificar quebre de ondas em águas rasas. O método usa a série temporal da elevação da superfície local e cria uma nova série temporal calculada a partir do espectro de energia local usando a transformada *wavelet* (ondaleta) do sinal de entrada que quantifica a presença de frequências tipicamente presentes em ondas arrebentando. Um experimento de laboratório em um canal de ondas irregulares foi conduzido e usado para testar o método em três regiões do canal, nas quais: (a) nenhuma onda estava arrebentando; (b) aproximadamente 30% das ondas estavam arrebentando; (iii) e a quase totalidade das ondas estavam arrebentando. O método foi testado estatisticamente na sua habilidade em identificar ondas arrebentando, com a ajuda do fato de que todas as ondas passando pelos pontos monitorados foram visualmente identificadas com arrebentando ou não-arrebentando. O método se mostrou acurado para a maioria dos casos e apenas falha quando a onda está na iminência de quebrar.

Palavras-chave: Arrebentação de ondas; Ondas irregulares; Análise de *wavelet*; Processos costeiros.

INTRODUCTION

In oceans, seas, lakes, reservoirs, estuaries, bays, etc., water wave breaking is probably the most significant phenomenon to happen in the nearshore hydrodynamics, having, among other effects, a strong influence in the nearshore currents and sediment transport. However, not very much is known about wave breaking in terms of prediction and modeling. The reason is because the hydrodynamics of a breaking wave is strongly turbulent, chaotic, perhaps even violating principles like the continuity of the fluid medium.

It is well accepted that wind-generated waves propagating to the coast are irrotational (Dean & Dalrymple, 1991). As the waves shoal on a beach slope, they tend to become steeper, more nonlinear, and to pitch forward as the particles at the crest start to move fast in comparison to the wave form itself (Flick et al., 1981). At this point the breaking process is beginning to take place and the motion very quickly turns from irrotational to extremely unstable and turbulent at the top front part of the wave crest eventually transferring much of the energy into small scale motions, sound waves, and heat (Deane et al., 2016). As breaking evolves, the wave height decreases, but the details, as well as a complete description of the process are still undergoing research. It is known however that the wave evolution during breaking depends on several factors, being the beach slope one of the most important. Authors (for example, Dean & Dalrymple,

1991) like to classify breaking waves into spilling, plunging and surging breakers. Spilling breakers take place in mild slope beaches, the surf zone (region where breaking occurs) usually extends for several wave lengths and the breaking process is very progressive. Plunging breakers occur on steeper beaches and are characterized by a narrow surf zone, and the wave crest curling and impinging on the trough. Surging breakers occur in very steep slopes where breaking itself is limited and strong reflection occurs.

In this work we develop an empirical method to identify breaking waves from a given time series of the free surface elevation entering the surf zone, breaking all the way to the swash region on the beach face. Of course, breaking can be visually identified because of the white capping at the crest and front of the wave/bore, so this identification can be used to testing a method that tries to identify breaking purely by operating on free surface elevation time series. We concentrate in spilling and plunging breaking waves, with negligible reflection. To both calibrate parameters and validate the method we performed a laboratory experiment described in a later section. Use of wavelets as a tool for the identification wave breaking inside the breaker zone is unknown to this author.

Wavelet analysis in coastal and ocean studies

The use of wavelets in ocean wave research that inspired this work was done by Liu (1994) to study applications of wavelets of offshore breaking waves as they are generated and propagate in deep waters. Similar application to breaking wavelets in deep water was performed by Mori & Yasuda (1994) and Liu & Babanin (2004).

Other ocean wave studies involving wavelets include the following. Wang et al. (2015) used wavelets for denoising and separating GPS measured waves. Liu et al. (2023) used wavelets with principal component analysis, among other methods, to study ocean wave modulation due to climate variability. Massel (2001) gives a general account of the power of wavelet analysis in characterizing wave spectra in several situations. Chuang et al. (2013) applied continuous wavelet transform to acceleration measure by a wave buoy to investigate noise and leakage in the process of reconstructing the free surface elevations. Lin & Liu (2004), Liu & Mori (2001), and Bayindir (2016). use wavelet analysis to identify and study freak (rogue) waves in deep water. Gemmrich (2005) reviews several different criteria of wave breaking, including wavelet analysis.

Here we present a very brief introduction to the wavelet equations as used in the paper.

One of the most useful mathematical tools in Engineering analysis is the so-called Fourier Transform, and it is defined, together with its inverse, as:

$$F(\omega) = \int_{-\infty}^{\infty} f(t) e^{-i\omega t} dt \tag{1}$$

$$f(t) = \frac{1}{2\pi} \int_{-\infty}^{\infty} F(\omega) e^{i\omega t} d\omega \tag{2}$$

where f is a continuous signal – in the present paper this is the displacement of the free surface as a time series, t is the independent variable in (1), and is usually time (as in this work) or space, F is the Fourier Transform of f, the complex amplitude of sinusoidal waves at each angular frequency ω, which is the independent variable in (2). Notice that this procedure requires knowledge of f in the entire t axis. If t is time, this means all past and future information. In practice, if f is measured data, we only have discrete values of f at certain values of t, and only for a finite interval of time. The discreteness of the signal can be overcome easily in most of the practical situations by the so-called discrete Fourier transform. The finiteness of the data set requires that we consider only the portion of data that we have and assume that it repeats to $\pm\infty$. The last assumption is equivalent to take the Fourier transform of a windowed signal, that is, the product of the signal with a window function that drops to zero at the end points. Alternatively, one can assume a form for the window that smooths the end points effects. The most relevant point (to the present work) about the Fourier transform, however, is that it cannot localize information. Any local feature of the data set will contribute to the whole spectrum (the spectrum is proportional to the square of the amplitude of F) despite its location in t.

Figure 1 illustrates this problem by showing two different signals, their Fourier spectra, and their wavelet spectra (see definition below). The signal on the left is a sum of three sinusoidal waves with different periods, the one on the right is composed of the same three waves, but in sequence. In both signals some random noise was also added. One can notice that the Fourier spectra for both signals are approximately the same, showing why the Fourier transform alone is only applicable to stationary data and cannot distinguish local features. To overcome this problem, Gabor (1946) proposed a Fourier transform with a narrow window (compared to the length of the time series) that translated along t, and this way it could be able to localize information around the center of the window. The problem with this procedure is that the size of the window being fixed, for relatively high frequencies, the window may be too broad to give good localization. The wavelet transform can resolve this problem. The wavelet transform is defined as

$$T(\tau, a) = \int_{-\infty}^{+\infty} \frac{f(t)}{\sqrt{a}} \left(\frac{t-\tau}{a} \right) dt \tag{3}$$

where f is the input signal (free surface time series) and ϕ is called the analyzing wavelet. a is a nondimensional scaling parameter. In this work we use the Morlet wavelet (Goupillaud et al., 1984), defined as:

$$\phi(t) = \pi^{-\frac{1}{4}} e^{-\frac{t^2}{2}} e^{-i\omega_0 t} \tag{4}$$

where ω_0 is a reference angular frequency.

Notice that the Morlet wavelet, when applied to (3) resembles a windowed Fourier transform with frequency $\sigma = \omega_0 / a$, and a window function that is "self-adjustable". In this paper we used a discretized version of Formula 3.

MATERIALS AND METHODS

The wavelet transform in the lower panel of Figure 1 shows its ability to detect the presence of nonstationary features in the signal. Figure 2 shows that, even for stationary signals, in this case an idealized sawtooth wave, the wavelet transform does remarkably

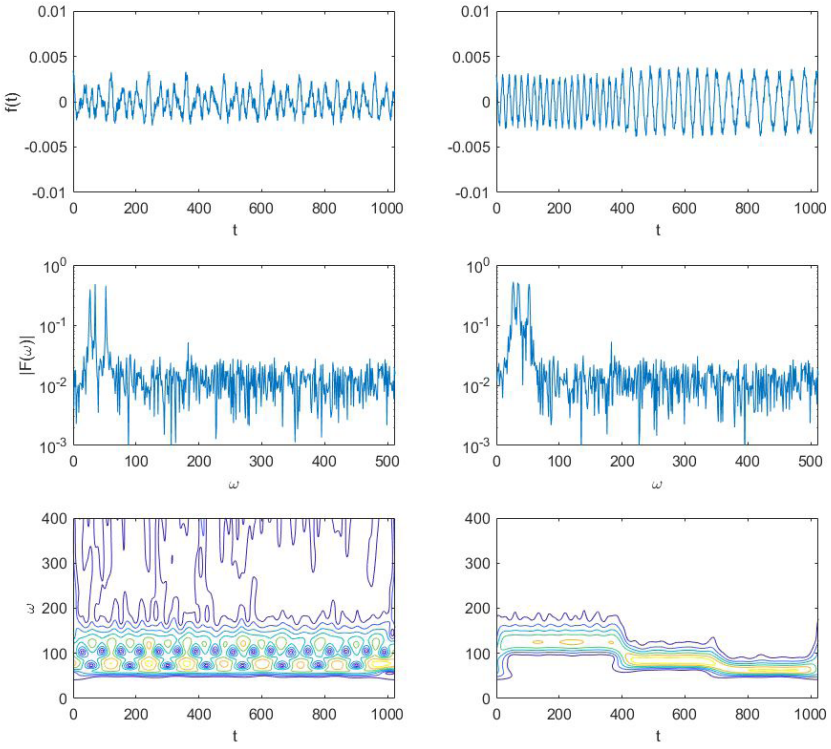

Figure 1. A stationary (top left) and a nonstationary (top right) time series, denoted as $f(t)$, their Fourier spectra (middle), and wavelet spectra (bottom).

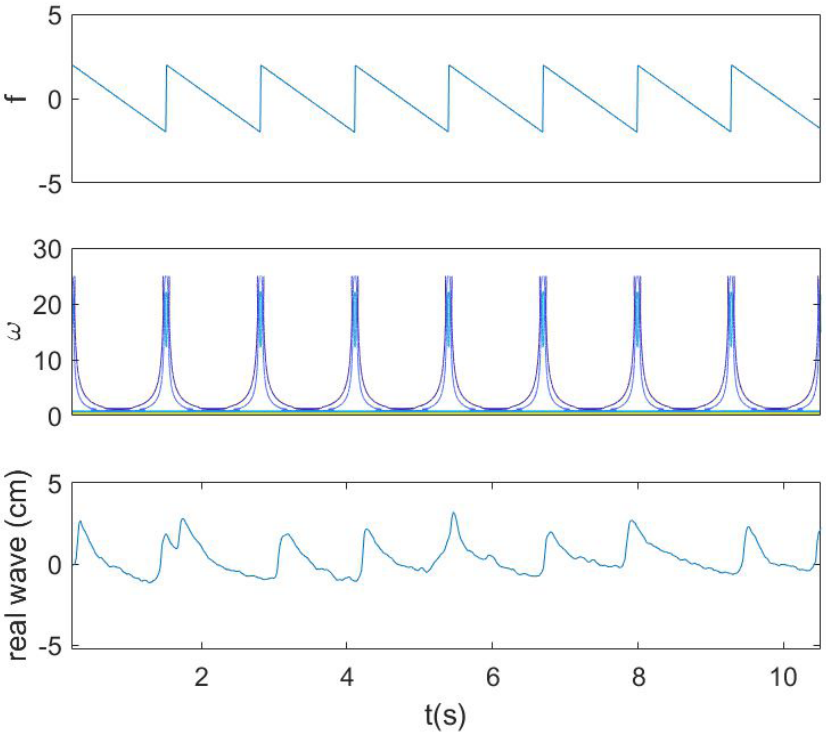

Figure 2. A breaking-wave-like idealized time series (top), its wavelet spectrum (middle), and a portion of breaking random waves measured at position "c".

well in localizing information. This example is a good indication that wavelet transform can be promising in studying wave breaking, since the sawtooth function is reminiscent of a real breaking wave train, as shown in the bottom plot of waves measured at position "c" of the experiment described in the next section.

Experimental setup

The experiment (Figure 3) was conducted with the wave flume in the Coastal Engineering Laboratory, at the University of Delaware by the present author and some collaborators. The tank's dimensions are 33 m long, 0.6 m wide, and 0.76 m tall, and an impermeable beach with arbitrary slope can installed at its far end. The waves are generated by a programmable hydraulic piston-type wavemaker capable of creating monochromatic sine waves, cnoidal waves, solitary waves, and random sea states. Measuring instruments are mounted on rails along any location along the tank. The set-up is adequate for studying a wide range of realistic unidirectional wave phenomena. The present experiment was performed with a 1:35 beach extending along the final three-quarters of the tank. A "deep water" depth of 40 centimeters was used and remained constant throughout the experiment. A first gauge (gauge g1 whose location is not shown in the figure) was located a few meters from the paddle to serve as a check for the generated wave train against the input to the wavemaker.

The experiment consisted of several runs with gauges g2, g3, g4, g5, g6 located at positions "a", "b", and "c" with several gauge spacings of 20 cm, 15 cm, 10 cm, and 5 cm. For the present paper however, only wave gauges 5 cm apart from each other, g5 (used for the actual computations of the method) and g6 (used as a check for consistency) were used. So, in summary we had experimental runs with gauges g5 and g6 at position "a", then the gauges were moved to position "b", and finally to position "c". Each run consisted of an identical set of random waves and lasted for twenty minutes. The tests began from a cold start to facilitate initial wave identification.

Position "a" was outside of the breaking region in deeper water where depth was around 39 cm and no breaking occurred. Position "b" was in a region where an estimate of 30% of the waves were breaking, with still water depth of around 13 cm. Position "c" was well inside the breaker zone, just before the swash zone, at 5 cm still water depth, and where nearly every wave was breaking. The data collection equipment consisted of voltage gauges connected to a datalogger and a computer. All surface elevation data were collected by the gauges at 50 hertz. A "fake gauge" g7 was set-up for a manual identification of breaking waves passing at gauge g5 for all runs at positions "a", "b", and "c". A voltage spike was sent to the datalogger by the pressing of a button by a human observer. Obviously, having 5 gauges at locations a, b and c with different spacings is redundant for the purpose of the present work and served only as a consistency/data quality check.

In what follows, we used the time series of gauge g5, spacing s2, at positions "a", "b", and "c" in the wave flume. For illustration purposes, the amplitude spectrum of the generated input waves, and the first few minutes of that input wave train, as well as waves at positions "a", "b", and "c", are shown in Figure 4.

The idea of the method is to create a time series that can identify waves that are breaking at the location, then compare the results with the breaking waves visually identified and recorded with gauge g7.

Method to identify breaking

It is well known that breaking waves have quite energetic high frequency harmonics. The idea is to find a frequency parameter σ_b which measures how elongated is the tail of the local energy spectrum of the wave, which can be conveniently nondimensionalized by the local peak frequency σ_p of the same spectrum. The other obvious measure associated with shoaling/breaking is the ratio $k_A = A/h$ of wave amplitude A to the still water depth h. Combinations of these parameters can be used as the index κ:

$$\text{(I) } \kappa = \frac{\sigma_b}{\sigma_p} \text{ or (II) } \kappa = \frac{A}{h} \text{ or (III) } \kappa = \frac{A}{h}\frac{\sigma_b}{\sigma_p} \tag{5}$$

and establish a necessary condition for wave is breaking if

$$\kappa \geq \kappa_b \tag{6}$$

where κ_b is a to-be-specified threshold. (5) and (6) are not meant to be a sufficient criterion for breaking, as very near-breaking waves may contain as much high frequency energy as a breaking wave. Nevertheless, waves meeting this condition will be either breaking or on the verge of breaking. Of the 3 proposals for κ in (5), tests showed that fore suitable choices of κ_b, results for (5-I) and (5-III) were comparable and much superior to (5-II),

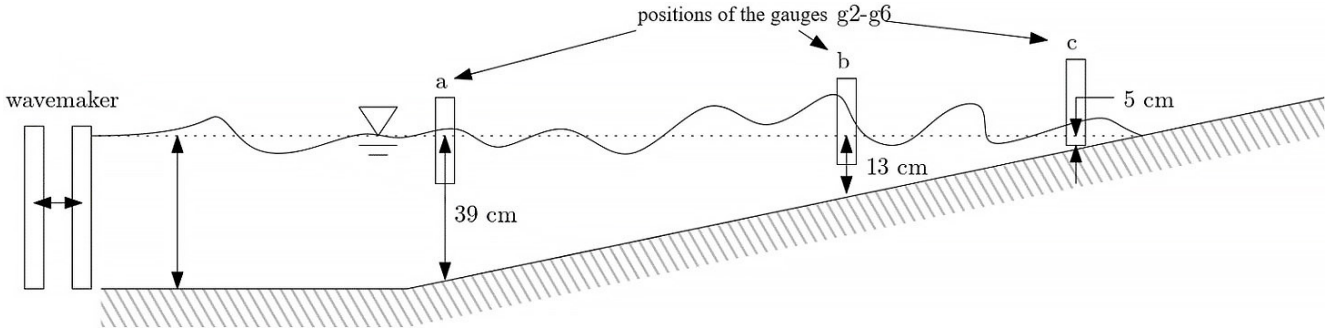

Figure 3. Wave flume schematics of the experimental set-up.

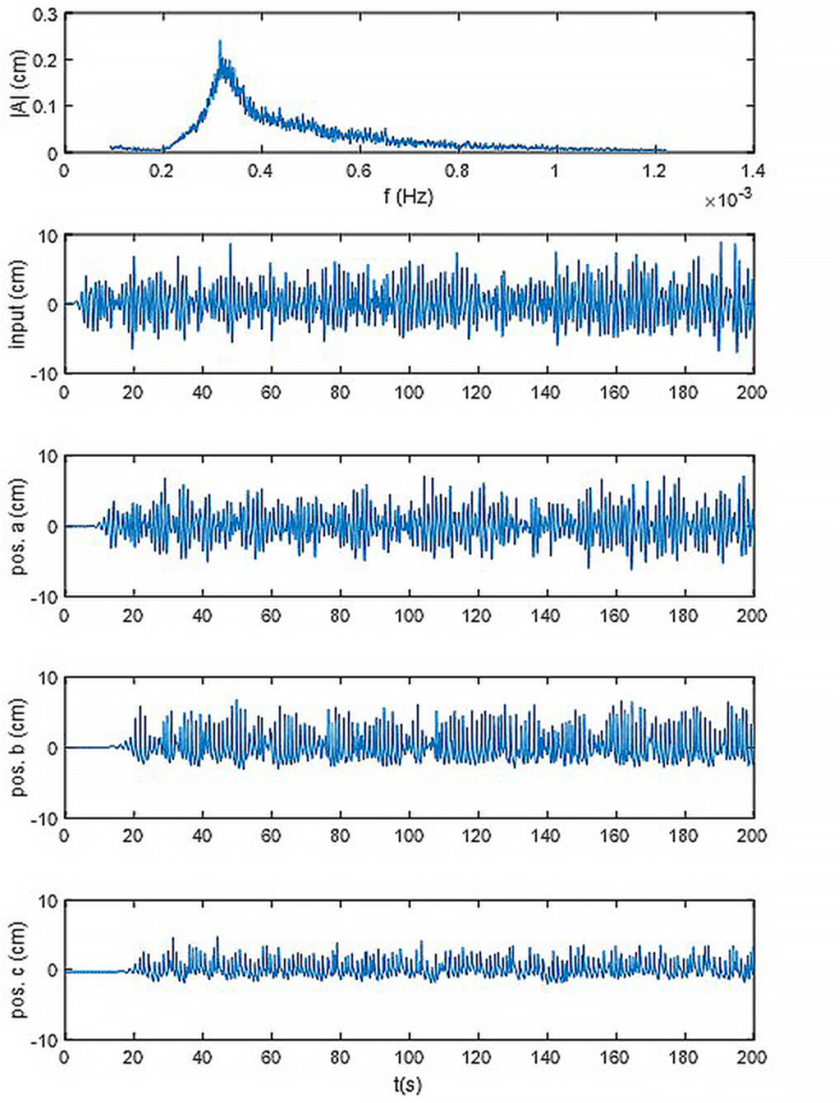

Figure 4. Amplitude spectrum of input waves (top) and initial portion (first 200 seconds out of a 20-minute total) of surface elevation recorded by the input gauge g1, and gauge g5 at positions "a", "b", and "c".

which is quite often used for regular waves. In the remaining of this we only show results using (5-III) formula for κ.

For monochromatic waves, the determination of the amplitude is rather immediate, but for a random wave train, it is necessary to filter out the phase of the wave and keep the envelope as the amplitude. This is done by taking the absolute value of the Hilbert transform $H\{f\}$ of the free surface elevation signal $f(t)$:

$$A(t) = H\{f\}(t) = \frac{1}{\delta}\int_{-\infty}^{\infty} \frac{f(\delta)}{t-\delta} d\tau \tag{7}$$

The parameter σ_b we propose is a such that its square is the centroid of the squared frequency of the portion of the power spectrum to the right of the energy peak. It is calculated using the wavelet transform as (Liu, 1994):

$$\sigma_b(t) = \left(\frac{\int_{\lambda\sigma_p}^{\sigma_N} \sigma^2 |T|^2 \, d\sigma}{\int_{\lambda\sigma_p}^{\sigma_N} |T|^2 \, d\sigma} \right)^{1/2} \tag{8}$$

where $|T|$ is the absolute value of the wavelet transform viewed as a function of σ (via $a \equiv \omega_0 / \sigma$) and $\tau \equiv t$, σ_p is the peak frequency of the spectrum at each t. λ is an adjusting factor greater equal to one (we used $\lambda = 1$), and σ_N is the highest frequency to be considered (e.g. the Nyquist frequency).

It should be mentioned that waves were identified and counted by the zero-up-crossing method, which picks-up a wave each time the free surface position crosses the still water level from negative to positive value.

Evaluation metrics

For the evaluation of the method, we present below statistical metrics that are particularly useful for binary situations such as the present one. We shall call "true positive" (TP), cases for which the method correctly predicted that a wave was breaking. The "false positive" (FP) as the predictions of non-breaking waves when they were breaking. The "true negative" (TN), when the method correctly predicts a non-breaking wave as non-breaking. The "false negative" (FN) as the incorrect prediction that a breaking wave was not breaking.

The metrics that we shall use are listed below:

- Accuracy: the measure of all the correctly identified cases (TP, FP, TN, FN). It is useful when all the classes of prediction are equally important. The formula is:

$$\text{Accuracy} = (\text{TP} + \text{FP}) / (\text{TP} + \text{FP} + \text{TN} + \text{FN}) .$$

- Precision: measure of the correctly identified positive cases from all the predicted positive cases. useful when "false positives" have high cost. The formula is:

$$\text{Precision} = \text{TP} / (\text{TP} + \text{FP}) .$$

- Recall: measure of the correctly identified positive cases from the sum of the actual positive cases. It is a convenient metric in situations where the cost of "false negatives" is high. The formula is:

$$\text{Recall} = \text{TP} / (\text{TP} + \text{FP}) .$$

- F1-score: this is the harmonic mean between Precision and Recall and is considered a better metric than the Accuracy. The formula is:

$$\text{F1\_score} = 2 \times (\text{Precision} \times \text{Recall}) / (\text{Precision} + \text{Recall}) .$$

RESULTS AND DISCUSSION

Figures 5, 6 and 7 show short portions of the time series for positions "a", "b", and "c", respectively. Each figure shows 2 blocks of 4 plots with the free surface time series – the waves for 2 neighboring gauges (5 and 6 – notice they are nearly identical), the identified breaking waves (gauge g7), the κ index time series corresponding to gauge 5, and the wavelet transform of gauge 5 (as a time varying power spectrum). For each individual wave, the value of κ is checked against the visually observed breaking record. A critical value of $\kappa_b = 4$ was established as the minimum κ value for breaking and it is marked on the κ plot. If the visually confirmed breaking wave corresponds to $\kappa \geq \kappa_b$, the method hits its target as successful. Similarly, when the wave is not breaking, the method works if, for that wave $\kappa < \kappa_b$. Otherwise, if a nonbreaking wave gets $\kappa \geq \kappa_b$ or a breaking wave gets $\kappa < \kappa_b$, the method missed (failed) that wave. We can compute statistically significant quantities to check the accuracy of the method. Notice in Figure 5 that for the time interval shown, no breaking was observed, and no breaking was identified by the method. This held true in position "a" for the entire duration of the experiment.

To compute the total number of waves in the time series, the zero-up crossing method was used. However, as this method has some ambiguities for random waves, in the sense that if applied at points slightly separated in space, it can give different number of waves, we used an average number of waves computed from other three gauges that were used in the same set of experiments. The total number of waves was estimated as 1100, but of course will vary slightly for each of the three positions "a", "b", and "c".

The number of breaking waves visually observed at position "b" was 28% of the total number of waves. It should be emphasized that the results to come are not general. They are valid for the time series studied here. However, they should be good for a similar random sea state as the parameters used are nondimensional. For this position "b", the method correctly predicted 254 breaking waves. The method also predicted 109 non-breaking was as breaking, and failed to predict 22 breaking waves, that is, the method in this case, predicted 22 breaking waves as non-breaking.

For the incoming waves in position "a", the method correctly indicated non-breaking waves for the entire time series.

For the swash zone waves (position "c"), there were 944 breaking waves, all of which the method predicted as breaking. However, the method also predicted 253 non-breaking waves as breaking.

We now present the counts for the statistical metrics presented in the preceding section. Table 1 summarizes the counts for each of the situations considered.

For the position "b" breaking zone, the method clearly has an unfortunate large number of "false positives". This can be attributed to the fact that. these waves probably fall in a category of what we are calling "waves on the verge of breaking". These waves, very probably, broke at a position only a few centimeters beyond the "b" position, and, since breaking waves were visually identified by the presence of "white caps" at the exact "b" position, they were not counted as breaking waves. The reason why these waves were identified as breaking by the present method, is because these imminently broken waves have as energetic higher harmonics (if not more) as a breaking wave. In fact, in the process of breaking, the wave is even losing some of its high frequency energy to turbulence, sound, and heat.

The statistical metrics *Accuracy*, *Precision*, *Recall* and *F1-score*, as presented in the preceding section, are shown in Table 2 the for the method's performance when applied to waves at positions "a", "b", and "c" (Table 1), and the aggregated result for the three positions considered together. All four presented metrics can vary from 0 (100% fail) to 1 (100% success). Notice that there is no *Precision*, *Recall*, or *F1-score* statistics for position "a". This is because the method never triggered "breaking" for the "deeper water" non-breaking waves, which is correct, but those three

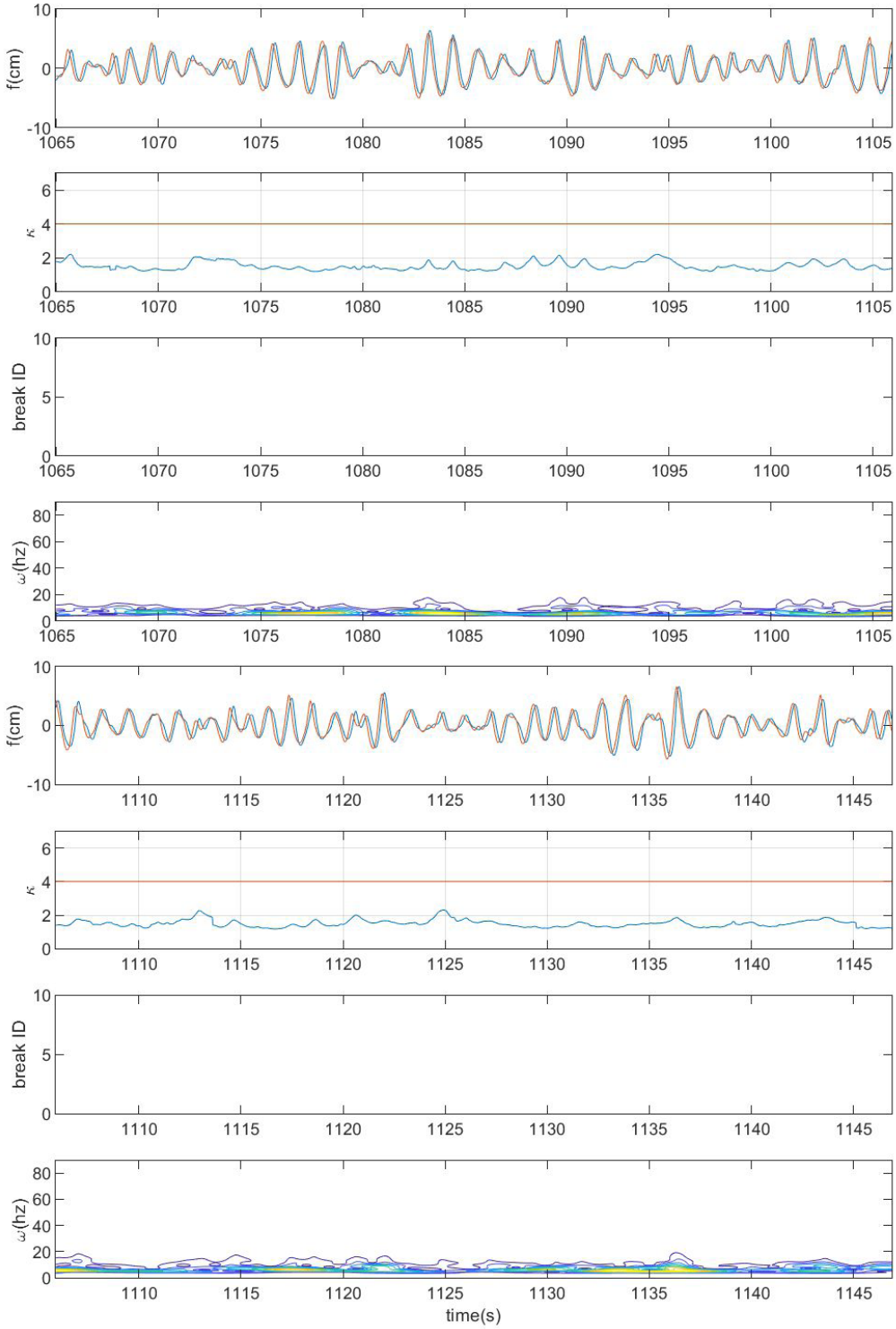

Figure 5. Position "a" (deep zone), from top to bottom, 2 blocks with 4 plots per block showing: portion of the time series for gauges g5 and g6; the visual breaking identification series (gauge g7); the corresponding computed breaking criterion parameter κ, and the corresponding wavelet computation of the time series. Notice that no waves are breaking for this entire interval.

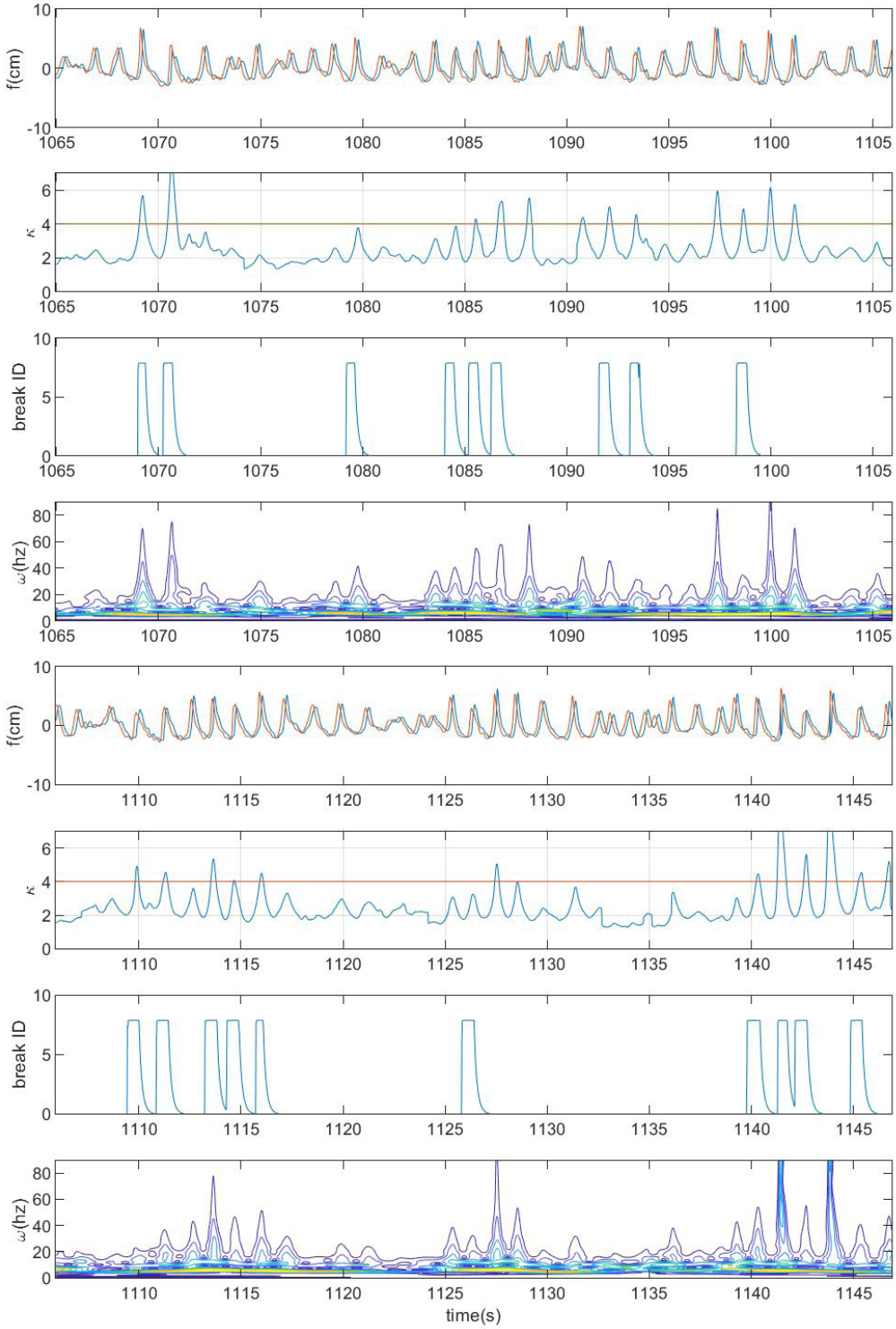

Figure 6. Position "b" (breaker zone), from top to bottom, 2 blocks with 4 plots per block showing: portion of the time series for gauges g5 and g6; the visual breaking identification series (gauge g7); the corresponding computed breaking criterion parameter κ, and the corresponding wavelet computation of the time series. Notice that about 30% of the waves are breaking.

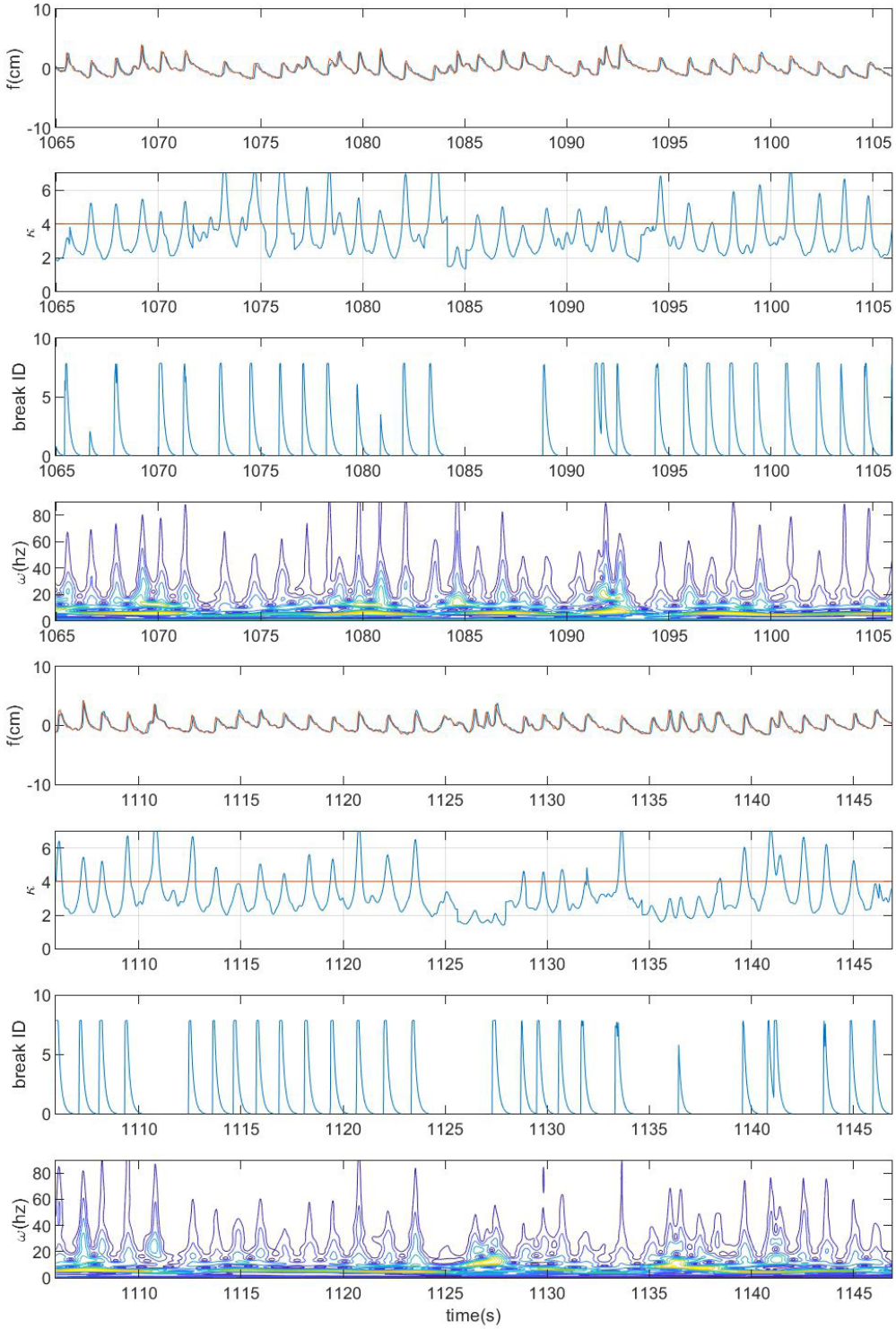

Figure 7. Position "c" (bore/swash zone), from top to bottom, 2 blocks with 4 plots per block showing: portion of the time series for gauges g5 and g6; the visual breaking identification series (gauge g7); the corresponding computed breaking criterion parameter κ, and the corresponding wavelet computation of the time series. Notice that about 90% of the waves are breaking.

Table 1. Counts of true positives, false positives, true negatives, false negatives.

	position "a"	position "b"	position "c"	total
TP	0	254	944	1198
FP	0	109	144	253
TN	1100	715	156	1827
FN	0	22	12	22

Table 2. Accuracy, precision, recall, and F1-score results for waves at: position "a" (incoming unbroken waves), position "b" (surf zone), and position "c" (near swash zone). The aggregated results for all gauge positions are shown as well.

	position "a"	position "b"	position "c"	total
Accuracy	1	0.881	0.869	0.917
Precision	-	0.699	0.867	0.826
Recall	-	0.920	1	0.982
F1-score	-	0.795	0.929	0.897

scores fail to exist in such situations. The accuracy, however, is 100% in those cases (not a useful result, though).

It is quite clear that the method is quite promising in the identification of breaking waves, particularly in regions where most waves are breaking (which is the case in most of the breaking zones on real coasts). It is also clear that the method tends to overestimate the number of breaking waves (prediction non-breaking waves as breaking – false-positives).

CONCLUSION

In general, the method works quite well for identifying breaking waves in a time series of surface elevation in coastal waters. However, the method was only applied for waves propagating in a single direction normal to the shore. Other experiments are necessary to ensure that the method is applicable to directional spectra, and it will likely require a parameterization of the breaking index that will depend on the incident angle.

For more extreme cases the method works very well, that is: for offshore locations where waves are not breaking, or in regions where nearly all waves are breaking, such as the bore and swashing regions, the method will not fail in identifying breaking. The method misses the most at locations where waves are on the verge of breaking. In those situations, the method tends to overestimate the number of breaking waves, because waves that are in the imminence of breaking will be identified as breaking because of its high frequency energy content. This should not be a problem because for practical purposes these waves will certainly break almost immediately after the observation as they are running up the shoreface.

By no means, the proposed study is completely conclusive and other formulas, parameters, wavelet functions, and limits for the breaking index k deserve investigation in other situations and scales. Tests with simpler wave trains could help in better understanding the significance of each variable derivable from the time series in the breaking process, and therefore provide enough information for a better calibration of the parameters involved in the method, or even a modification the method itself.

ACKNOWLEDGEMENTS

The author wants to thank the following people at the Coastal Engineering Laboratory of the University of Delaware where the laboratory experiment was conducted, particularly James Kirby, Arun Chawla, Kirk Bosma, Michael Herrman.

REFERENCES

Bayindir, C. (2016). Early detection of rogue waves by the wavelet transforms. *Physics Letters A*, *380*(1-2), 156-161. http://doi.org/10.1016/j.physleta.2015.09.051.

Chuang, L. Z.-H., Wu, L.-C., & Wang, J. H. (2013). Continuous wavelet transform analysis of acceleration signals measured from a wave buoy. *Sensors*, *13*(8), 10908-10930. PMid:23966188. http://doi.org/10.3390/s130810908.

Dean, R. G., & Dalrymple, R. A. (1991). Water wave mechanics for engineers and scientists. *Advanced Series on Ocean Engineering*, *2*, http://doi.org/10.1142/1232.

Deane, G. B., Stokes, D., & Callaghan, A. H. (2016). Turbulence in breaking waves. *Physics Today*, *69*(10), 86-87. http://doi.org/10.1063/PT.3.3339.

Flick, R. E., Guza, R. T., & Inman, D. L. (1981). Elevation and velocity measurements of laboratory shoaling waves. *Journal of Geophysical Research*, *86*(C5), 4149-4160. http://doi.org/10.1029/JC086iC05p04149.

Gabor, D. (1946). Theory of communication. *Journal of the Institution of Electrical Engineers – Part III: Radio and Communication Engineering*, *93*(26), 429-457.

Gemmrich, J. (2005). On the occurrence of wave breaking. In *Proceedings of the 14th 'Aha Huliko'a Hawaiian Winter Workshop on Rogue Waves* (pp. 123-130). University of Hawai.

Goupillaud, P., Grossmann, A., & Morlet, J. (1984). Cycle-octave and related transforms in seismic signal analysis. *Geoexploration*, *23*(1), 85-102. http://doi.org/10.1016/0016-7142(84)90025-5.

Lin, E., & Liu, P. C. (2004). A discrete wavelet analysis of freak waves in the ocean. *Journal of Applied Mathematics*, *2004*(5), 379-394. http://doi.org/10.1155/S1110757X0430611X.

Liu, J., Meucci, A., & Young, I. R. (2023). A comparison of multiple approaches to study the modulation of ocean waves due to climate variability. *Journal of Geophysical Research. Oceans*, *128*(9), e2023JC019843. http://doi.org/10.1029/2023JC019843.

Liu, P. C., & Babanin, A. V. (2004). Using wavelet spectrum analysis to resolve breaking events in the wind wave time series. *Annales Geophysicae*, *22*(10), 3335-3345. http://doi.org/10.5194/angeo-22-3335-2004.

Liu, P. C., & Mori, N. (2001). Wavelet spectrum of freak waves in the ocean. *Coastal Engineering*, *2000*, 1092-1098. http://doi.org/10.1061/40549(276)84.

Liu, P. (1994). Wavelet spectrum analysis and ocean wind waves. In E. Foufoula-Georgiouand & P. Kumar (Eds.), *Wavelets in geophysics* (pp. 151-166). San Diego: Academic.

Massel, S. R. (2001). Wavelet analysis for processing of ocean surface wave records. *Ocean Engineering*, *28*(8), 957-987. http://doi.org/10.1016/S0029-8018(00)00044-5.

Mori, N., & Yasuda, T. (1994). Orthonormal wavelet analysis for deep-water breaking waves. In *Proceedings of 24th Conference on Coastal Engineering* (Vol. 1, pp. 412-426), Kobe, Japan. ASCE.

Wang, J., He, X., & Ferreira, V. G. (2015). Ocean wave separation using CEEMD-wavelet in GPS wave measurement. *Sensors*, *15*(8), 19416-19428. PMid:26262620. http://doi.org/10.3390/s150819416.

Authors contributions

Mauricio Felga Gobbi: Conducted the study, data organization, analysis and writing of the article.